Article:
Smith, Olivia A.M., Nashed, Youssef S.G., Duncan, Christian et al. (3 more authors) (2020) 3D Modeling of craniofacial ontogeny and sexual dimorphism in children. Anatomical Record. ISSN: 1932-8494

https://doi.org/10.1002/ar.24582

3D Modelling of Craniofacial Ontogeny and Sexual Dimorphism in Children

Olivia A. M. **Smith**[1], Youssef S.G. **Nashed**[4], Christian **Duncan**[2], Nick **Pears**[3], Antonio **Profico**[5] , Paul **O'Higgins**[1, 5]

1. Hull York Medical School, University of York, York, UK, YO10 5DD
2. Dept. of Plastic Surgery, Alder-Hey Hospital, Liverpool, UK, L12 2AP
3. Department of Computer Science, University of York, York, UK YO10 5GH
4. Stats Perform, Chicago, IL, USA, 60601;
5. PalaeoHub, Dept. of Archaeology, University of York, York, UK YO10 5DD

Corresponding author:

Paul O'Higgins, BSc, MBBS, PhD, DSc
PalaeoHub,
Dept. of Archaeology and Hull York Medical School,
University of York,
York,
UK
YO10 5DD
paul.ohiggins@hyms.ac.uk
tel:+44 1904 328872

Financial Disclosure Statement: The authors have no interests to disclose

Short Running Head:

Craniofacial ontogeny and sexual dimorphism

Grant sponsor(s): __0_____; Grant number(s): ___0_____.

Abstract:

Background

The range of normal variation of growth and development of the craniofacial region is of direct clinical interest but incompletely understood. Here we develop a statistical model of craniofacial growth and development to compare craniofacial ontogeny between age groups and sexes and pilot an approach to modelling that is relatively straightforward to apply in the context of clinical research and assessment.

Methods

The sample comprises head surface meshes captured using a 3dMD five-camera system from 65 males and 47 females (range 3-20 years) from the *Headspace* project, Liverpool, UK. The surface meshes were parameterised using 16 anatomical landmarks and 59 semilandmarks on curves and surfaces. Modes and degrees of growth and development were assessed and compared among ages and sexes using Procrustes based geometric morphometric methods.

Results

Regression analyses indicate that 3-10 year olds undergo greater changes than 11-20 year olds and that craniofacial growth and development differs between these age groups. The analyses indicate that males extend growth allometrically into larger size ranges, contributing substantially to adult dimorphism. Comparisons of ontogenetic trajectories between sexes find no significant differences, yet when hypermorphosis is accounted for in the older age group there is a significant residual sexual dimorphism.

Conclusions.

The study adds to knowledge of how adult craniofacial form and sexual dimorphism develop. It was carried out using readily available software which facilitates replication of this work in diverse populations to underpin clinical assessment of deformity and the outcomes of corrective interventions.

Keywords: Human facial growth; 3D scanning; Morphometrics; Sexual Dimorphism

Introduction:

Craniofacial surgery aims to correct congenital and acquired deformities by realigning patients with the 'normal' population. To achieve this, knowledge of the range of normality and a means by which patients can be assessed against this are essential. Our aim in this paper is to develop a statistical model of whole head surface variation based on individuals living in the UK of both sexes, ranging in age from 3-20 years. We explore the extent and nature of changes in the size and shape of the head in this age range, comparing early and later stages of growth and development and assess sexual dimorphism in the sample.

Anthropometry of facial soft and hard tissues, has a long history in studies of craniofacial biology and plastic and reconstructive surgery (Howells, 1973; O'Higgins et al., 1990; Farkas, 1994). In craniosynostosis surgery, the cranial index derived from calliper measurements of skull maximum width expressed as a percentage of maximum length is commonly used. Although this is easily measured and repeatable, it captures limited aspects of cranial form and can be misleading as an outcome measure. Such approaches suffer several mensurational and statistical issues (Moyers and Bookstein, 1979; Rohlf, 2000) and are not useful in regions with few recognizable landmarks.

To address this, using 3D surface images, correspondences of points among surface meshes are frequently computed using a template landmark configuration close to the average of the population (Blanz and Vetter, 1999), with or without user-specified, anatomically-equivalent landmarks (Paysan et al., 2009). The template is then morphed to the set of surfaces to be landmarked. Examples include the Non-rigid Iterative Closest Points (NICP) algorithm (Amberg et al., 2007) and the Coherent Point

Drift (CPD) algorithm (Myronenko and Song, 2010). A recent approach trains a statistical shape model of the human head (Dai et al., 2018), combining CPD with a methodology that employs 'as-rigid-as-possible' deformations (Sorkine and Alexa, 2007) to iteratively locate landmarks. This is similar to the sliding semilandmark technique from Geometric Morphometrics (GM), applied in the present study because it explicitly seeks to map developmental homologies. In this, anatomical landmarks guide the 'sliding' of semilandmarks over curves and surfaces to minimise 'bending energy' (local 'error' in semilandmark placement; see Methods).

Once surface meshes have been parameterised as sets of corresponding landmarks, models of variation can be derived and used to assess other surface meshes. These generally use approaches based on estimations of shape or size and shape distances derived from generalised Procrustes analysis, principal components analysis and other multivariate methods, as is common in GM studies (Dai et al., 2020).

In the paediatric population, assessment of craniofacial form is complicated by dynamic, continuous growth changes. Since congenital craniofacial abnormalities are typically surgically corrected early in childhood, it is vital that surgeons have access to an age and sex appropriate 3D craniofacial model pre- and post-operatively. Currently, there is no widely accepted objective measure of paediatric craniofacial normality. A precise understanding of human ontogeny and sex differences that arise during childhood is essential for generating such a model, and so to understanding craniofacial pathologies and their correction.

Between birth and adulthood, sexual dimorphism of craniofacial form becomes apparent. Dimorphic differences between adult male and female soft tissue faces (Dai et al., 2020; Ploumpis et al., 2020) and the craniofacial skeleton are well described

(Bulygina et al., 2006; Franklin et al., 2007; O'Higgins et al., 1990; Rosas and Bastir, 2002). Principally, males are noted to have prominent chins, jaw angles, supraorbital and nasal regions and relatively reduced cheeks as well as being larger than females. Typically, these changes are linked to hormone associated growth differences with males, for the most part, extending growth and so, form change, relative to females during late puberty. Sex differences have been noted at varying subadult ages; 3 years (Kesterke et al., 2016), 4.7years (Gaži-Čoklica et al., 1997), 6 years (Ferrario et al., 1999) and 14 years (Koudelová et al., 2015) with a recent study (Matthews, 2018) claiming the presence of sexual dimorphism in children as early as 1 year.

This study revisits the issues of ontogenetic and sexual variation in craniofacial form using an approach to landmarking and analysis that explicitly respects homology. This ensures that the underlying (distance) metric relates to biologically meaningful differences. We characterise postnatal ontogenetic changes in size and shape and investigate the ontogeny of sexual dimorphism, comparing our findings with those of previous studies. Through this study we demonstrate the efficacy of a statistically and biologically valid approach to such work that can be readily replicated in clinical research using commonly available and inexpensive software tools. These have significant potential in pre- and post-operative surgical management.

Methods:

Ethics approval:

Ethics approval was granted by Alder-Hey Hospital and The Hull York Medical School. Written informed consent was gained from all volunteers, or their legal guardian if <18years. Consent was to allow the 3D photography of their heads to provide data to

assess normal head variation. We confirm adherence to the tenets of the Declaration of Helsinki.

Sample:

The sample comprises Wavefront™ .obj head surface meshes (typically 180K vertices and approx. 360K triangles) from 65 males and 47 females (range 3-20 years; Table 1). These were chosen from the sample collected by the *Headspace* (see 'Software, tools and data availability') project in Liverpool from September 2013 – January 2014 using a 3dMD five-camera system to capture head geometry. All participants wore smooth, tight fitting latex caps to flatten the hair closely to the scalp. Individuals who had previous craniofacial surgery, declared mixed or unknown ethnicity, bulky hair or errors in their surface data were excluded, thus limiting sources of error as far as possible and focussing on growth within the indigenous local population.

Digitisation:

Developmentally homologous landmarks, curves and surfaces were digitised using an algorithm devised by Bookstein and Green (Bookstein and Green, 1994). This was further developed (Gunz and Mitteroecker, 2013) and incorporated in the EVAN Toolbox for geometric morphometrics (Weber and Bookstein, 2011), which was used in this study.

A template was created in the EVAN Toolbox comprising 16 anatomical landmarks (Table 2) and an exemplar head surface mesh with traced curves marked up by 59 semilandmarks. The semi-landmark configurations represented the right and left jawlines, the right and left eyebrows and the midline, as well as the surface between curves and landmarks (Fig. 1). To facilitate subsequent interpretation of asymmetry, the template was rendered symmetrical using the method of reflected relabelling

(Mardia et al., 2000). Semilandmarks were then warped and projected from the template onto each parent curve or surface in each individual using a triplet of thin plate splines (Bookstein, 1989). The semilandmarks were then slid along curves and over the surface to minimise the bending energy of the thin plate splines with respect to the anatomical landmarks (Bookstein, 1989; Gunz and Mitteroecker, 2013). The full set of 16 anatomical landmarks and 59 semilandmarks was used as the basis of subsequent statistical analyses.

Statistical analyses:

The analyses examined growth (changes in size and shape), development (changes in shape over time) and ontogenetic transformation as a whole (changes in size and shape over time) from 3-20 years. For subsequent analyses centroid size (the square root of the sum of squared distances between each landmark and the centroid) was used as measure of scale, and the shape variables are the landmark and semilandmark coordinates after generalised Procrustes analysis (GPA). Analyses of form (shape and size; Mitteroecker et al., 2013) use these shape variables plus the natural logarithm of centroid size (ln csize) .

Changes were assessed for the whole sample using principal components analysis (PCA) and modelled using multivariate regressions, both computed using the EVAN Toolbox. The regressions were repeated for younger (3-10 years) and older (11-20 years) subjects and the directions of regression vectors were compared using a permutation test on the angles between them (using the R package Arothron (Profico et al., 2015). Additionally, regressions and tests of angles were repeated for each sex alone. Finally, residual sexual differences in shape from these regressions, after

adjusting all individuals to mean age or centroid size, were assessed for significance using a permutation test. The results of these analyses were visualised by warping the template surface mesh between the landmarks and semilandmarks of pairs of surfaces (from the 'reference' to the 'target') derived by warping along principal components or multivariate regression vectors of interest. To facilitate interpretation of how each target surface differs from its reference, the surface mesh was converted into a colour map, representing the change in area of each triangle of the surface mesh between these, using the MapAreaDist in the R package, Arothron (Piras et al., 2020).

Results

Between 3 and 20 years, centroid size and age are strongly associated (Fig. 2; whole sample $r = 0.84$; males $r = 0.88$; females $r = 0.87$; all $p < 0.00001$). Males and females largely overlap, although the oldest males attain greater centroid sizes than females. Additionally, the youngest males appear somewhat smaller than the youngest females leading to the impression that growth vectors may differ but the angle between the sex specific vectors of size regressed on age is not significantly different from 0 (29^0, permutation test $p = 0.69$).

A principal components analysis of shape (the coordinates after GPA) was carried out for the whole sample. In Fig. 3., males and females overlie each other except at the positive limit of PC1 where males exceed females in density. Warping of the mean to the limits of PC1 (Fig. 3, insets lower frame) indicates that the shape changes it represents are similar to what we would expect of development, with heads more typical of young adults plotting towards the positive extreme of PC1. Older females tend to have lower PC1 scores than older males, indicating that their morphology is more juvenile-like than that of similarly aged males.

A second PCA of form (shape variables plus ln centroid size) is presented in Fig. 4. As in the PCA of shape (Fig. 3), the positive limit of PC1 shows a greater density of males than females and the warped mean closely resembles the changes in size and shape that would be expected of growth and development, with larger more mature looking individuals plotting towards the upper limit of PC1. As in Fig. 3, older females have lower PC1 scores than older males.

In both PCAs there is a suggestion of curvilinearity of ontogenetic trajectories with a change in vector near 10 years of age in higher PCs (PC4, shape; PC5, form, not shown). In Fig. 2, males below 10 years tend to be smaller than females, and larger above 10 years. Additionally, many previous studies have indicated that growth of the head shifts from being dominated by changes in the neurocranium earlier in development and in the face, later. For these reasons we divided the sample into two age cohorts, 3-10 years and 11-20 years, to assess the extent to which ontogenetic vectors change over time.

The results of the multivariate regressions of shape on size, shape on age and form on age are presented in Table 3. These were calculated for combined sexes 3-20 years, combined sexes 3-10 years and 11-20 years as well as sexes separately for ages 3-10yrs and 11-20 years. All are highly significant ($p<001$), indicating that the sample as whole and each subsample shows significant ontogenetic changes in form over time. The % of total variance in shape, explained by the regression of shape on ln centroid size in the 3-10 year olds is ~1.5 times as great as that in the 11-20 year olds. Similarly, for the regression of shape on age almost twice as much variance is explained in the younger age group and for form on age, more than twice.

The significance of angles between the regression vectors of ontogenetic change in size and shape from Table 3 and are presented in Table 4. In every comparison between age groups there is a significant difference, indicating different allometries, developments and so, ontogenies. The warpings of Fig. 5 indicate that between the ages of 3 and 10 years, changes in head form mainly comprise expansions of the orbital and nasal regions with accompanying smaller expansions in the regions of the cheeks and chin. These contribute to vertical increase in facial height and nasal protuberance. Between the ages of 11 and 20 the focus of facial expansion shifts inferiorly, being concentrated around the lips and chin, which become more prominent.

Over the whole period 3-20 years and within each of the age subgroups, there is no significant difference between sexes in the directions of their ontogenetic vectors (Table 4). Table 5 presents further analyses of sexual dimorphism that test the significance of differences (Procrustes shape or form distances). A permutation test is applied after allometric adjustment of each individual by multivariate regression to mean ln centroid size or to ages 7.5 years for the younger, and 15.5 years for the older age groups. Multivariate regression was based on pooled sexes, because the previous analyses (Table 4) showed their vectors do not differ. These tests indicate that there are no significant residual sex differences in shape in the younger age group but, in the older age group, differences are highly significant. The Procrustes form distance between the means of males and females adjusted to age 15.5 (0.0164) is approximately 25% of the total form difference (0.064) between sexes aged 19 and 20 years. The Procrustes shape distance (0.0164) between the means of sexes adjusted to the mean ln centroid size is a little over half the total sex shape distance (0.028) for 19-20 year olds.

Therefore, these residual aspects of sexual dimorphism are small but not unimportant relative to the component of form difference arising from hypermorphosis. They are shown in Fig. 6, magnified by a factor of 10 to facilitate visualisation. After regression adjustment, males relative to females have a more vertically elongated and narrow head. Females possess relatively larger lips and nasal bridge with a more rounded, shorter chin, relatively smaller jaw angles and a philtrum that is less prominent. These differences are common to, but not equally marked in the residuals from the two regressions, indicating that age and size related changes in shape are not quite coincident in the older age groups.

Discussion

Our analyses find no difference in the rate of growth (change in size with age) between sexes but indicate that the oldest males are larger than the oldest females (Fig 2). Regarding shape and form variation, both PCAs (Fig. 3 and 4) indicate that a substantial contributor to young adult craniofacial sexual dimorphism is hypermorphosis; males extend a common trajectory of growth and development into larger size ranges with shape scaling allometrically. These findings reflect similar results from previous studies of soft tissue faces (Kesterke et al., 2016) and the craniofacial skeleton (Bulygina et al., 2006; Franklin et al., 2008; O'Higgins et al., 1990; Rosas and Bastir, 2002).

Regression analyses (Table 2) indicate that growth and development are relatively greater sources of variation among 3-10 year olds than among 11-20 year olds. Further, age appears marginally better than size as a predictor of shape than size alone (ignoring allometric effects), which accounts for a major proportion of the observed ontogenetic changes in overall form with age. Angular comparisons of these

vectors (Table 4) find no difference in allometry (shape vs size), development (shape vs age), or in how form varies with age among sexes in either age group but very clear differences in all regression vectors between younger (below 10) and older (11-20) age groups.

How form changes with age in both age groups is visualised in Fig. 5. In the younger group, changes in head shape mainly comprise expansions of the orbital and nasal regions and to a lesser extent, the cheeks and chin, contributing to increased facial height and nasal protuberance. The focus of change shifts inferiorly between the ages of 11 and 20 to the region of the lips and chin, leading to their becoming more prominent. These findings are consistent with earlier work (Bastir et al., 2006; Enlow, 1968) that identified a maturation gradient which results in early completion of neurocranial growth, followed sequentially by the mid and lower face. The gradient likely reflects differences in rate and duration of growth between brain, bone and cartilage (Bastir et al., 2006) with vertical growth linked to intranasal cartilage expansions and chin prominence linked to continuing growth at the mandibular condyles (Enlow and Hans, 1996; Scott, 1954).

Finally, while allometric scaling as a consequence of male hypermorphosis underlies a significant proportion of sexual dimorphism in our sample, the regression analyses suggest that some proportion of sexual dimorphism is independent of scaling and temporal extension of growth in males (time hypermorphosis). These aspects are shown in Fig. 6. In this, the differences are magnified 10 times and consist of a more vertically elongated and narrow head in males relative to females and much larger lips and nasal bridge with a more rounded, shorter chin, relatively smaller jaw angles and philtrum in females. These sex differences are significant but the angle between regressions in each sex are insignificant, probably due to limitations of sampling,

particularly below 10 years. As such, we cannot determine if these differences arise early, in the neonatal period and are simply carried forward into adulthood, being added to by male hypermorphosis (Ferrario et al., 1999; Gaži-Čoklica et al., 1997; Kesterke et al., 2016; Koudelová et al., 2015), or have arisen through divergence of trajectories

The current work contributes to our understanding of how the head grows and develops and was carried out using the readily available Evan Toolbox and R based software for colour maps that is open source. Using these, this research can readily be extended to different populations. Further, with little development it is possible to envisage a semiautomatic tool for scanning and parameterising the heads of patients in the clinical setting with the aim of enhancing diagnosis and treatment of craniofacial growth disorders, as well as characterising site and extent of dysmorphology to enable both surgical planning and outcomes assessment.

Software, tools and data availability

The Headspace data are available via the project website, https://www-users.cs.york.ac.uk/~nep/research/Headspace/. Our VPN for the EVAN toolbox analyses are distributed via https://www.evan-society.org/; The template and data can be downloaded from https://doi.org/10.5281/zenodo.4266269;. The R tool for visualisation of differences in meshes is available on CRAN at https://CRAN.R-project.org/package=Arothron, the function is localmeshdiff.

References

Amberg, B., Romdhani, S., Vetter, T., 2007. Optimal step nonrigid ICP algorithms for surface registration, in: 2007 IEEE Conference on Computer Vision and Pattern Recognition. IEEE, pp. 1–8.

Bastir, M., Rosas, A., O'Higgins, P., 2006. Craniofacial levels and the morphological maturation of the human skull. J Anat 209, 637–654. https://doi.org/10.1111/j.1469-7580.2006.00644.x

Blanz, V., Vetter, T., 1999. A morphable model for the synthesis of 3D faces, in: Proceedings of the 26th Annual Conference on Computer Graphics and Interactive Techniques. pp. 187–194.

Bookstein, F.L., 1989. Principal warps: Thin-plate splines and the decomposition of deformations. IEEE Transactions on Pattern Analysis & Machine Intelligence 567–585.

Bookstein, F.L., Green, W.D., 1994. Edgewarp: A flexible program package for biometric image warping in two dimensions, in: Visualization in Biomedical Computing 1994. International Society for Optics and Photonics, pp. 135–147.

Bulygina, E., Mitteroecker, P., Aiello, L., 2006. Ontogeny of facial dimorphism and patterns of individual development within one human population. Am J Phys Anthropol 131, 432–443. https://doi.org/10.1002/Ajpa.20317

Dai, H., Pears, N., Smith, W., Duncan, C., 2020. Statistical Modeling of Craniofacial Shape and Texture. International Journal of Computer Vision 128, 547–571.

Dai, H., Pears, N., Smith, W., Duncan, C., 2018. Symmetric Shape Morphing for 3D Face and Head Modelling. Presented at the Automatic Face & Gesture Recognition (FG 2018), 2018 13th IEEE International Conference on, IEEE, pp. 91–97.

345 Enlow, D.H., 1968. The human face: an account of the postnatal growth and
346 development of the craniofacial skeleton. Hoeber Medical Division, Harper &
347 Row.
348 Enlow, D.H., Hans, M.G., 1996. Essentials of Facial Growth. W. B. Saunders
349 Company, Philadelphia.
350 Farkas, L.G., 1994. Anthropometry of the Head and Face. Raven Pr.
351 Ferrario, V.F., Sforza, C., Poggio, C.E., Schmitz, J.H., 1999. Soft-tissue facial
352 morphometry from 6 years to adulthood: a three-dimensional growth study
353 using a new modeling. Plastic and reconstructive surgery 103, 768–778.
354 Franklin, D., O'Higgins, P., Oxnard, C.E., 2008. Sexual dimorphism in the mandible of
355 indigenous South Africans: A geometric morphometric approach. S Afr J Sci
356 104, 101–106.
357 Franklin, D., Oxnard, C.E., O'Higgins, P., Dadour, I., 2007. Sexual dimorphism in the
358 subadult mandible: Quantification using geometric morphometrics. J Forensic
359 Sci 52, 6–10. https://doi.org/10.1111/j.1556-4029.2006.00311.x
360 Gaži-Čoklica, V., Muretić, Ž., Brčić, R., Kern, J., Miličić, A., 1997. Craniofacial
361 parameters during growth from the deciduous to permanent dentition—a
362 longitudinal study. European journal of orthodontics 19, 681–689.
363 Gunz, P., Mitteroecker, P., 2013. Semilandmarks: a method for quantifying curves and
364 surfaces. Hystrix, the Italian journal of mammalogy 24, 103–109.
365 Howells, W.W., 1973. Cranial variation in man. Papers of the Peabody Museum of
366 Archaeology and Ethnology, Harvard University 67. Cambridge. Mass.
367 Kesterke, M.J., Raffensperger, Z.D., Heike, C.L., Cunningham, M.L., Hecht, J.T., Kau,
368 C.H., Nidey, N.L., Moreno, L.M., Wehby, G.L., Marazita, M.L., 2016. Using the

3D Facial Norms Database to investigate craniofacial sexual dimorphism in healthy children, adolescents, and adults. Biology of sex differences 7, 23.

Koudelová, J., Brůžek, J., Cagáňová, V., Krajíček, V., Velemínská, J., 2015. Development of facial sexual dimorphism in children aged between 12 and 15 years: a three-dimensional longitudinal study. Orthodontics & craniofacial research 18, 175–184.

Mardia, K.V., Bookstein, F.L., Moreton, I.J., 2000. Statistical assessment of bilateral symmetry of shapes. Biometrika 285–300.

Matthews, H.S., 2018. Changing the face of craniofacial growth curves: modelling growth and sexual dimorphism in children and adolescents using spatially dense 3D image analysis.

Mitteroecker, P., Gunz, P., Windhager, S., Schaefer, K., 2013. A brief review of shape, form, and allometry in geometric morphometrics, with applications to human facial morphology. Hystrix 24, 59–66. https://doi.org/10.4404/hystrix-24.1-6369

Moyers, R.E., Bookstein, F.L., 1979. The inappropriateness of conventional cephalometrics. American journal of orthodontics 75, 599–617.

Myronenko, A., Song, X., 2010. Point set registration: Coherent point drift. IEEE transactions on pattern analysis and machine intelligence 32, 2262–2275.

O'Higgins, P., Moore, W.J., Johnson, D.R., McAndrew, T.J., Flinn, R.M., 1990. Patterns of cranial sexual dimorphism in certain groups of extant hominoids. Journal of Zoology 222, 399–420.

Paysan, P., Knothe, R., Amberg, B., Romdhani, S., Vetter, T., 2009. A 3D face model for pose and illumination invariant face recognition, in: 2009 Sixth IEEE International Conference on Advanced Video and Signal Based Surveillance. Ieee, pp. 296–301.

Piras, P., Profico, A., Pandolfi, L., Raia, P., Di Vincenzo, F., Mondanaro, A., Castiglione, S., Varano, V., 2020. Current options for visualization of local deformation in modern shape analysis applied to paleobiological case studies. Frontiers in Earth Science 8, 66.

Ploumpis, S., Ververas, E., O'Sullivan, E., Moschoglou, S., Wang, H., Pears, N., Smith, W., Gecer, B., Zafeiriou, S.P., 2020. Towards a complete 3D morphable model of the human head. IEEE Transactions on Pattern Analysis and Machine Intelligence.

Profico, A., Veneziano, A., Melchionna, M., Piras, P., Raia, P., 2015. Arothron: R functions for geometric morphometrics analyses. R package version 314.

Rohlf, F.J., 2000. On the use of shape spaces to compare morphometric methods. Hystrix, the Italian Journal of Mammalogy 11, 9–25.

Rosas, A., Bastir, M., 2002. Thin-plate spline analysis of allometry and sexual dimorphism in the human craniofacial complex. American Journal of Physical Anthropology 117, 236–245. https://doi.org/10.1002/ajpa.10023

Scott, J.H., 1954. The growth of the human face. Proceedings of the Royal Society of Medicine 47, 91–100.

Sorkine, O., Alexa, M., 2007. As-rigid-as-possible surface modeling, in: Symposium on Geometry Processing. pp. 109–116.

Weber, G.W., Bookstein, F.L., 2011. Virtual Anthropology - A Guide for a New Interdisciplinary Field. Springer-Verlag, Wien.

Legends for figures

Figure 1: top row, left: The fixed landmarks (see Table 1), curves and surface measured on each head. Top row, right: the same landmarks, curves and surfaces with semilandmarks. Bottom row: frontal and lateral views of a fully parameterised head.

Figure 2: Growth of the head; Females, black circles, Males, crosses.

Figure 3: PCA of shape using the whole sample, ages 3-20. PC1 accounts for 32% of the total variance and PC2 for 11%. Females, black circles, Males, crosses.

Figure 4: PCA of form using the whole sample, ages 3-20. PC1 accounts for 77% of the total variance and PC2 for 4%. Females, black circles, Males, crosses.

Figure 5: Visualisation of the changes from 3-10-20 years (left, middle, right) from multivariate regression of form (shape and size) on age. The head colour maps indicate the relative expansion or contraction in the area of surface regions between 3 and 10 years (middle) and between 11and 20 years (right).

Figure 6: Visualisations of residual sex dimorphism in shape (differences between sex means) after warping all individuals between 11 and 20 years to age 15.5 years (top) and to ln of the mean centroid size (bottom). The warping of each head from the sex mean is exaggerated by a factor of 5 and so the differences between heads appear 10x greater than in reality.

Table legends:

Table 1: Individuals included in this study by age and sex

Table 2: Definitions of fixed facial landmarks

Table 3: Multivariate regressions of shape on ln centroid size and age, and of form on age within each age group with sexes separate and combined. All regressions are significant as assessed using a permutation test.

Table 4: Comparisons of ontogenetic trajectories from multivariate regressions of shape on ln centroid size and age, and of form on age. The magnitudes and significances of the angles between trajectories are presented for comparisons between age groups and sexes. Significance was assessed using a permutation test, significant differences in bold.

Table 5: The degree and significance of sexual dimorphism in shape in each age group before and after adjusting data to mean ln centroid size or ages, 7.5 years (3-10 age group), 15.5 years (11-20 age group). Dimorphism is quantified using distances, D, which are Procrustes shape distances (upper row) and Procrustes form distances (lower row). Significance was assessed using a permutation test, significant differences in bold.

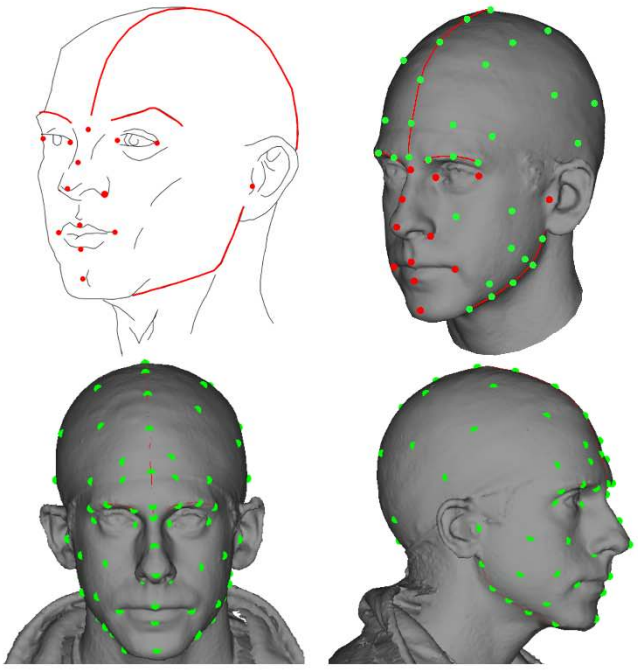

Figure 1: top row, left: The fixed landmarks (see Table 1), curves and surface measured on each head. Top row, right: the same landmarks, curves and surfaces with semilandmarks. Bottom row: frontal and lateral views of a fully parameterised head.

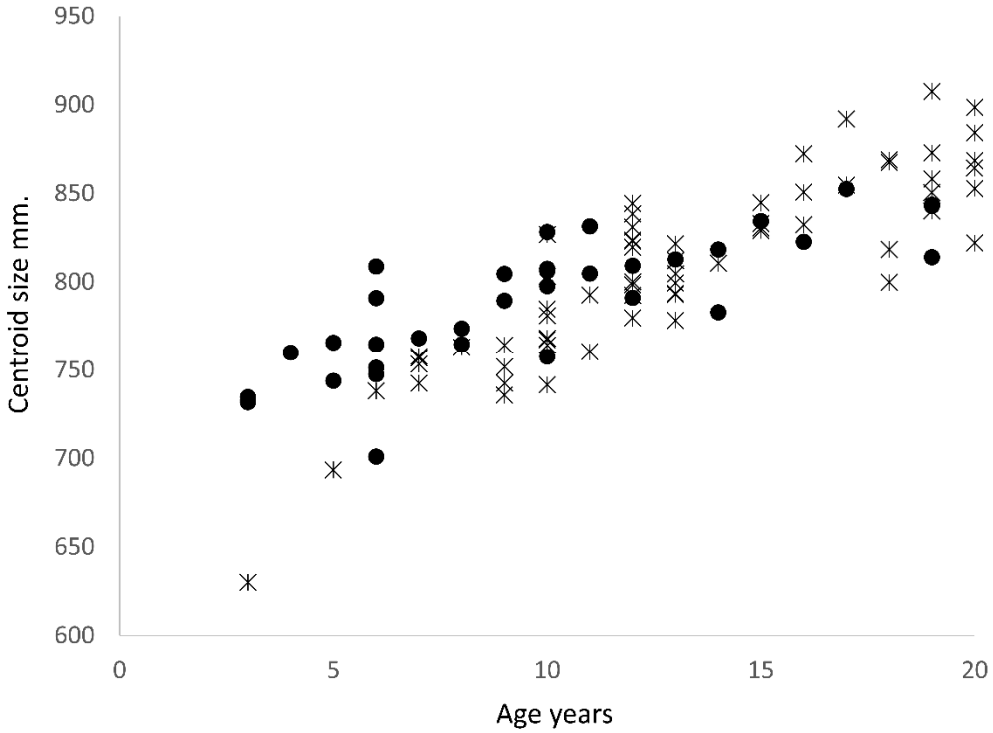

467

468 **Figure 2:** Growth of the head; Females, black circles, Males, crosses.

469

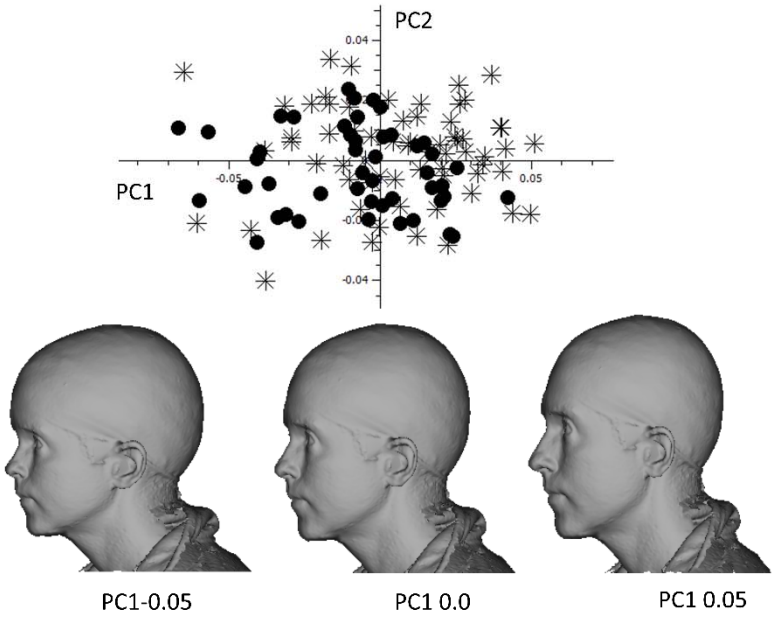

Figure 3: PCA of shape using the whole sample, ages 3-20. PC1 accounts for 32% of the total variance and PC2 for 11%. Females, black circles, Males, crosses.

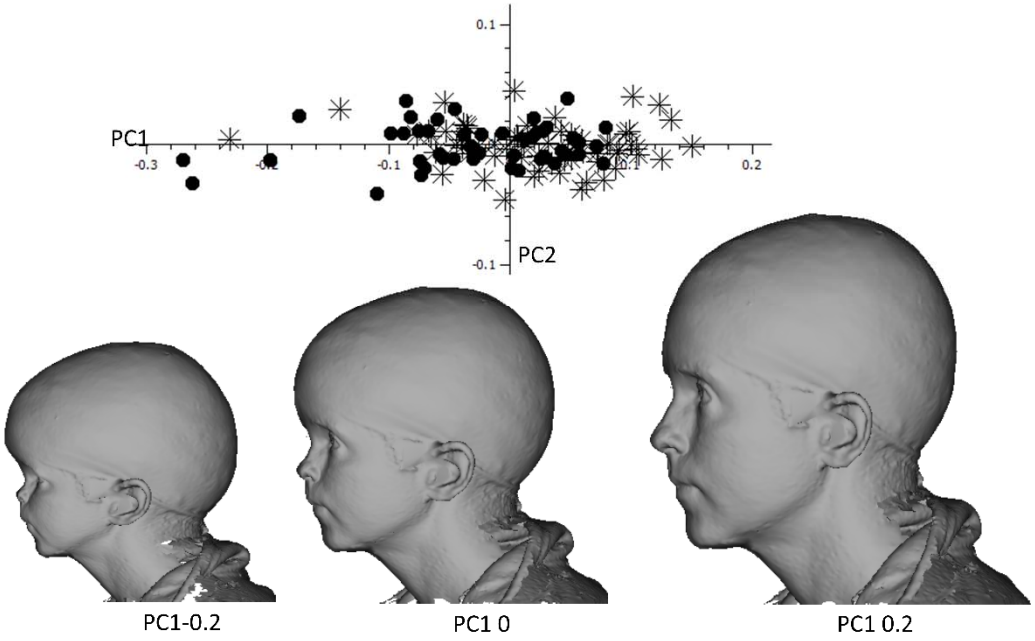

474

475 **Figure 4:** PCA of form using the whole sample, ages 3-20. PC1 accounts for 77% of

476 the total variance and PC2 for 4%. Females, black circles, Males, crosses.

477

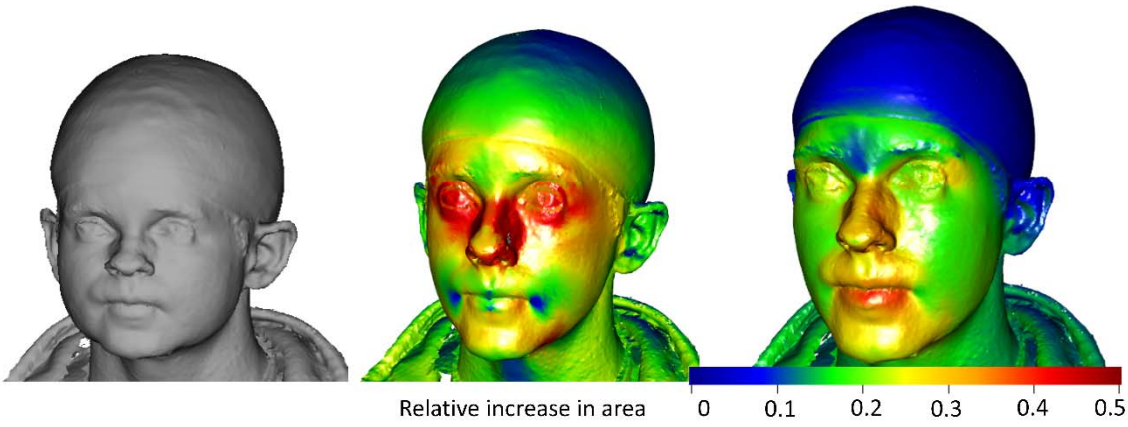

478

479 **Figure 5:** Visualisation of the changes from 3-10-20 years (left, middle, right) from
480 multivariate regression of form (shape and size) on age. The head colour maps
481 indicate the relative expansion or contraction in the area of surface regions between
482 3 and 10 years (middle) and between 11and 20 years (right).

483

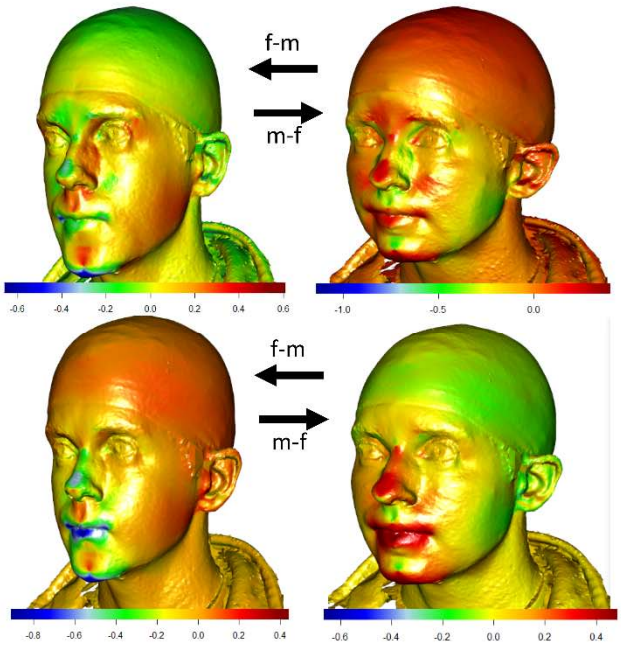

484

485 **Figure 6:** Visualisations of residual sex dimorphism in shape (differences between sex
486 means) after warping all individuals between 11 and 20 years to age 15.5 years (top)
487 and to ln of the mean centroid size (bottom). The warping of each head from the sex
488 mean is exaggerated by a factor of 5 and so the differences between heads appear
489 10x greater than in reality.

490

Age Yrs.	f	m
3	3	1
4	1	
5	2	1
6	6	1
7	1	4
8	2	2
9	2	4
10	5	8
11	3	2
12	2	10
13	1	7
14	2	1
15	1	4
16	1	3
17	1	2
18		4
19	8	5
20	6	6

Table 1: Individuals included in this study by age and sex

No.	Landmark definition
1 & 3	Medial canthus
2 & 4	Lateral canthus
5	Nasal bridge
6	Middle of nose
7	Tip of nose
8 & 9	Corner of mouth
10	Middle of cupid’s bow upper lip
11	Middle of bottom lip
12	Tip of chin
13 & 14	Tragus
15 & 16	Lateral nasal alar rim

Table 2: Definitions of fixed facial landmarks

Multivariate regressions	n	Shape v Ln centroid Size		Shape v age		Form v age	
		(% Var. exp.)	*significance p*	*(% Var. exp.)*	*significance p*	*(% Var. exp.)*	*significance p*
Combined sexes 3-20	112	20.04	<0.001	20.89	<0.001	56.06	<0.001
Combined sexes 3-10	43	12.76	<0.001	16.79	<0.001	49.23	<0.001
3-10 male	21	16.95	<0.001	19.47	<0.001	47.36	<0.001
3-10 female	22	13.78	<0.002	19.9	<0.001	46.35	<0.001
Combined sexes 11-20	69	9.03	<0.001	9.83	<0.001	21.25	<0.001
11-20 male	44	9.88	<0.001	14.4	<0.001	32.38	<0.001
11-20 female	25	9.41	0.003	10.66	<0.001	27.57	<0.001

Table 3: Multivariate regressions of shape on ln centroid size and age, and of form on age within each age group with sexes separate and combined. All regressions are significant as assessed using a permutation test.

Ontogenetic vector comparisons between ages 3-10 and 11-20	**Shape vs. size**		**Shape vs. age**		**Form vs age**	
	angle^{o}	**P**	**angle^{o}**	**p**	**angle^{o}**	**p**
3-10 female vs 11-20 female	72	**<0.001**	64	<0.001	27	**<0.001**
3-10 female vs 11-20 male	53	**<0.001**	48	<0.001	21	**<0.001**
3-10 male vs 11-20 male	62	**<0.001**	67	<0.001	29	**<0.001**
3-10 male vs 11-20 female	69	**<0.001**	78	<0.001	33	**<0.001**
combined sexes 3-10 vs 11-20	49	**<0.001**	61	<0.001	26	**<0.001**
between the sexes						
3-20 female vs 3-20 male	23	0.379	22	0.223	8	0.195
3-10 female vs 3-10 male	48	0.417	45	0.181	17	0.264
11-20 female vs 11-20 male	47	0.181	43	0.278	21	0.561

Table 4: Comparisons of ontogenetic trajectories from multivariate regressions of shape on ln centroid size and age, and of form on age. The magnitudes and significances of the angles between trajectories are presented for comparisons between age groups and sexes. Significance was assessed using a permutation test, significant differences in bold.

Sexual dimorphism	age 3-10		age 11-20	
	D	p	D	p
Shape adjusted to mean ln centroid size	0.00963	0.888	0.0164	**0.004**
Form adjusted to 7.5/15.5 years	0.01061	0.752	0.0164	**0.001**

Table 5: The degree and significance of sexual dimorphism in shape in each age group before and after adjusting data to mean ln centroid size or ages, 7.5 years (3-10 age group), 15.5 years (11-20 age group). Dimorphism is quantified using distances, D, which are Procrustes shape distances (upper row) and Procrustes form distances (lower row). Significance was assessed using a permutation test, significant differences in bold.